EUROPEAN ORGANIZATION FOR NUCLEAR RESEARCH

CERN - PS DIVISION

CERN/PS 2002-054 (AE)
CLIC Note 527

LUMINOSITY LIMITATIONS AT THE MULTI-TeV LINEAR COLLIDER ENERGY FRONTIER

D. Schulte

Abstract

To achieve the desired high luminosity in e^+ e^- linear colliders with centre-of-mass energies above the TeV scale, careful optimisation of the beam parameters is necessary. Constraints arising from the RF structure design, the beam-beam interaction, the damping ring and the beam delivery system have to be taken into account and compromises between different requirements have to be found. The nature of these different constraints is discussed and the resulting limits for the luminosity are detailed.

Presented at the 8th European Particle Accelerator Conference, 3-7 June, 2002, Paris, France

Geneva, Switzerland
25 July 2002

LUMINOSITY LIMITATIONS AT THE MULTI-TeV LINEAR COLLIDER ENERGY FRONTIER

D. Schulte, CERN, Geneva, Switzerland

Abstract

To achieve the desired high luminosity in e^+e^- linear colliders with centre-of-mass energies above the TeV scale, careful optimisation of the beam parameters is necessary. Constraints arising from the RF structure design, the beam-beam interaction, the damping ring and the beam delivery system have to be taken into account and compromises between different requirements have to be found. The nature of these different constraints is discussed and the resulting limits for the luminosity are detailed.

1 INTRODUCTION

Already at a centre-of-mass energy of $E_{cm} = 500\,\mathrm{GeV}$, a linear collider can complement the experimental results from LHC [1]. Higher energies would allow for an even wider reach. Since many cross sections are proportional to E_{cm}^{-2}, very high luminosities are required at multi-TeV energies. The CLIC study (for Compact Linear Collider) at CERN is investigating the possiblity of realising such a collider [2].

In a linear collider, the two beams are created in injectors and their transverse emittances are reduced in damping rings. The beams are then compressed longitudinally in bunch compressors before they are accelerated in the main linacs. Then they are collimated and focused to very small spot sizes in the beam delivery system (BDS); finally they collide in the interaction point (IP). Many components of a linear collider are technically challenging and can put severe constraints on the machine design. This paper can certainly not do justice to all those components. It will concentrate on a few subsystems that are some of the main drivers for the overall design. These are the damping rings, the main linacs, the BDS and the beam-beam interaction.

As a simplified approach, the luminosity $\mathcal{L}$ in such a collider is a function of the effective transverse beam sizes at the IP, σ_x and σ_y, and the number of particles per bunch N

$$\mathcal{L} \propto H_D \frac{N}{4\pi\sigma_x\sigma_y}\eta P \qquad (1)$$

Here, P is the total power consumption of the linac and η is the efficiency to turn this power into beam power. H_D is the luminosity enhancement factor due to the beam-beam interaction. It is usually in the range 1–2. The transverse RMS beam sizes may be larger than the effective ones because the beams can develop significant tails. As an example, the main parameters of CLIC at $E_{cm} = 3\,\mathrm{TeV}$ can be found in Table 1.

Table 1: Basic parameters of CLIC at $E_{cm} = 3\,\mathrm{TeV}$.

Parameter	symbol	value
luminosity in the peak [$\mathrm{cm}^{-2}\mathrm{s}^{-1}$]	$\mathcal{L}_1$	3×10^{34}
pulses per second	f_{rep}	$100\,\mathrm{Hz}$
bunches per pulse	n_b	154
bunch separation	Δt	$0.67\,\mathrm{ns}$
particles per bunch	N	4×10^9
hor. beam size at IP	σ_x	$65\,\mathrm{nm}$
vert. beam size at IP	σ_y	$0.7\,\mathrm{nm}$
bunch length at IP	σ_z	$35\,\mu\mathrm{m}$
norm. hor. emittance before BDS	ϵ_x	$0.68\,\mu\mathrm{m}$
norm. vert. emittance before BDS	ϵ_y	$10\,\mathrm{nm}$

The different sub-systems put constraints on the parameters of equation 1. As will be shown, the beam-beam interaction sets a fundamental lower limit on σ_x as a function of N and σ_z. The damping ring and the beam delivery system also give a lower limit to σ_x. Static and dynamic imperfections in the damping ring, main linac and beam delivery system give a lower limit to the vertical spot size σ_y. The efficiency is determined by the main linac. In the following, the beam-beam effect is treated first, then come the beam delivery system, the main linac and the dynamic effects. In the end, limitations from the damping ring are mentioned.

The transverse emittances vary along the machine: in the case of CLIC, the target values for the damping rings are $\epsilon_x = 450\,\mathrm{nm}$ and $\epsilon_y = 3\,\mathrm{nm}$; and $\epsilon_x = 600\,\mathrm{nm}$ and $\epsilon_y = 5\,\mathrm{nm}$ after the bunch compression. At the end of the main linac, $\epsilon_x = 680\,\mathrm{nm}$ and $\epsilon_y = 10\,\mathrm{nm}$ is aimed at; the effective emittances at the IP should be $\epsilon_x \approx 1700\,\mathrm{nm}$ and $\epsilon_y \approx 20\,\mathrm{nm}$. Simulations that combine the effects of the main linac and the beam-beam interaction showed that the reduction in luminosity caused by a very small emittance growth can be large [3]. However this will be ignored here for simplicity and because the effect is much smaller for the CLIC parameters.

2 BEAM-BEAM EFFECTS

To achieve the desired high luminosity, the beams have to be focused to very small transverse sizes at the IP. Each bunch thus creates a strong electromagnetic field which focuses the oncoming bunch. This reduces the transverse sizes of the beams during collision and leads to an increased luminosity. Because the particles' trajectories are bent, they emit beamstrahlung which is similar to synchrotron radiation. With some probability, colliding particles therefore have lost some energy. This leads to the development of a luminosity spectrum, which usually still

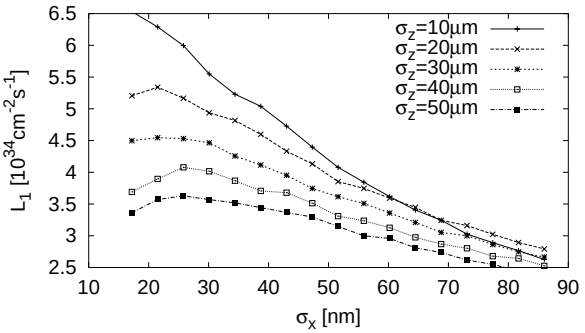

Figure 1: The luminosity in the peak as a function of the horizontal spot size, simulated for CLIC with GUINEA-PIG [6]. Beamstrahlung effect and coherent pair creation are taken into account.

has a peak at the nominal centre-of-mass energy. For most physics experiments, only the high energy fraction of the luminosity spectrum is of interest. We will thus use $\mathcal{L}_1$, defined as the luminosity with $E_{cm} > 0.99E_{cm,0}$; in CLIC we have $\mathcal{L}_1 \approx 0.3\mathcal{L}$. The hardness of the beamstrahlung can be described by the beamstrahlung parameter Υ which depends on the critical energy ω_c of the beamstrahlung and the beam energy E_0 as $\Upsilon = 2/3\hbar\omega_c/E_0$. For Gaussian beams the average value is $\langle\Upsilon\rangle \approx 5/6Nr_e^2\gamma/(\alpha(\sigma_x + \sigma_y)\sigma_z)$ [5]; α is the fine structure constant and r_e the classical electron radius. High luminosity at high energy necessitates $\langle\Upsilon\rangle \gg 1$, CLIC has $\langle\Upsilon\rangle \approx 8$

Reducing σ_x leads to higher luminosity but also to a higher number of beamstrahlung photons. Colliding particles are more likely to have lost energy. For large Υ and $\sigma_x \gg \sigma_y$, one needs to use $\sigma_x \propto N\sqrt{\sigma_z}$ to stay in the optimum and consequently

$$\mathcal{L}_1 \propto \frac{\eta P}{\sigma_y\sqrt{\sigma_z}} \tag{2}$$

Figure 1 shows $\mathcal{L}_1$ for $N = 4 \times 10^9$ and $\sigma_y = 0.7\,\mathrm{nm}$ as a function of σ_x.

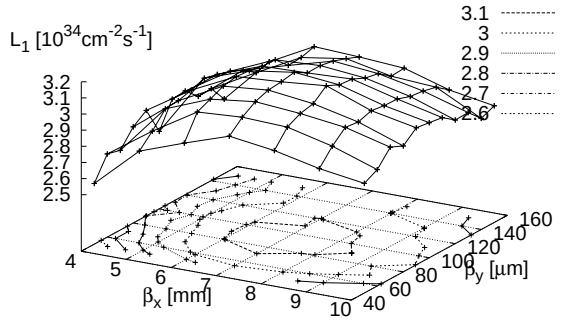

Figure 2: The luminosity $\mathcal{L}_1$ in CLIC as a function of the horizontal and vertical beta-functions for $\epsilon_x = 680\,\mathrm{nm}$ and $\epsilon_y = 10\,\mathrm{nm}$ before the BDS.

Another important limitation arises from coherent pair production. A photon can decay into an electron-positron pair in a very strong electromagnetic field. This coherent pair creation depends strongly on Υ. For $\Upsilon \ll 1$, as in most linear colliders at $E_{cm} = 500\,\mathrm{GeV}$, it is strongly suppressed. At $\Upsilon \gg 1$ the production rate can be very significant. In CLIC one produces about 6×10^8 pairs per bunch crossing, corresponding to 15% of the bunch charge. Increasing Υ or n_γ enhances this effect. The coherent pairs have some impact on the beam-beam interaction; but most importantly their power is a significant fraction of the beam power and can create very high background levels or even destroys magnets. This problem has been studied inside the detector [4] but it needs further investigation.

3 BEAM DELIVERY SYSTEM

The BDS consists of a collimation section in which beam tails are scraped off and the final focus section that squeezes the beam to the required small spot size at the IP. Some diagnostics will also be included in this system. The small beam sizes at the IP are achieved by a combination of small emittances and beta-functions $\beta_{x,y}$, but the normally expected $\sigma_{x,y} = \sqrt{\epsilon_{x,y}\beta_{x,y}/\gamma}$ is not reached. The energy spread of the incoming beam is large ($\approx 1\%$ full width); in spite of a careful lattice design, full compensation of the chromaticity cannot be achieved. In addition, the beams emit synchrotron radiation in the bends, quadrupoles and multipoles. Due to the stochastic nature of the process, this leads to an increase of the beam size at the IP. A famous example of this process is the Oide effect [7]. Achieving very small beta-functions at the IP implies that the particles have large amplitudes in the final quadrupole doublet before the IP and likely emit synchrotron radiation. The changes in energy alter the effective focusing of the quadrupoles, leading to a spot size increase.

The final focus system of CLIC [8] is based on a design by P. Raimondi [9]. The nominal beta-functions at the IP are $\beta_x = 6\,\mathrm{mm}$ and $\beta_y = 70\,\mu\mathrm{m}$, with a spot size of $\sigma_x \approx 37\,\mathrm{nm}$ and $\sigma_y \approx 0.5\,\mathrm{nm}$ for the incoming emittances $\epsilon_x = 0.68\,\mu\mathrm{m}$ and $\epsilon_y = 10\,\mathrm{nm}$, when beam energy spread and synchrotron radiation are neglected.

Tracking through the BDS with PLACET [10] and simulating the beam-beam interaction with GUINEA-PIG yields a luminosity of $\mathcal{L}_1 = 5.5 \times 10^{34}\,\mathrm{cm}^{-2}\mathrm{s}^{-1}$. If energy spread and radiation are included, one finds $\mathcal{L}_1 = 3.2 \times 10^{34}\,\mathrm{cm}^{-2}\mathrm{s}^{-1}$. The reduction is mainly due to synchrotron radiation in the bends and the initial beam energy spread, while the Oide effect plays a minor role. The luminosity spectrum obtained can be well reproduced by assuming effective Gaussian bunch sizes $\sigma_x \approx 65\,\mathrm{nm}$ and $\sigma_y \approx 0.7\,\mathrm{nm}$ at the IP; the RMS spot sizes are much larger. Simulation of an incoming horizontal emittance $\epsilon_x = 0$ shows still an effective $\sigma_x \approx 40\,\mathrm{nm}$ at the IP. Tracking with varying ϵ_y shows the expected $\mathcal{L}_1 \propto 1/\sqrt{\epsilon_y}$ over a wide range. The BDS thus gives an important lower limit

to σ_x but not to σ_y.

The beta-functions have been determined without taking the beam-beam effect into account [8]. Repeating the above simulation for different β_x nad β_y shows that we are close to an optimum, see Fig. 2.

4 MAIN LINAC

While linacs using superconducting accelerating structures made of niobium should be able to reach very high efficiencies, their achievable gradient is limited. A higher gradient allows to have a more compact and therefore cheaper accelerator, or at the same price a higher energy reach. Within limits, normal conducting linacs should be able to reach higher gradients at higher RF frequencies f_{RF}. CLIC is therefore based on $f_{RF} = 30\,\mathrm{GHz}$ and a gradient $G = 150\,\mathrm{MV/m}$.

Two main problems at very high gradients are RF breakdowns of the structures and damage caused by the instantaneous heating of the structures during the RF pulse. Both problems are under study; different materials and structure geometries are being investigated. The final choice of acceleration frequency and gradient will depend on the outcome. For usual copper, it is anticipated that the RF breakdown problem can be solved by limiting the surface field to $\approx 300\,\mathrm{MV/m}$ [11]. This, and a reduction of the surface heating, can be more easily achieved at a small iris radius a, while for the luminosity, a larger a is advantageous. In the following, the implications of a given structure on the beam parameters are detailed. Then different structures will be compared.

4.1 Beam Current and Bunch Length

The efficiency η is the product of the efficiencies to turn power into RF power, which usually depends on the efficiencies of modulators and klystrons, and of the RF power to beam efficiency. Here we focus on the latter. The efficiency η depends on the beam current I, the gradient and the shunt impedence R roughly as $\eta \propto \frac{I}{\frac{G}{R}+I}$ For a given structure, one tries to maximise the beam current in the main linac, either by decreasing the seperation of bunches Δt or by increasing the number of particles per bunch N.

The most important lower limit of Δt arises from the emittance growth due to transverse multi-bunch wakefields. To reduce these wakefields the transverse modes in the structures are damped. In the case of CLIC, they are extracted from the structure using small waveguides that are terminated with a load to avoid reflection [12]. The chosen bunch-to-bunch distance is $0.67\,\mathrm{ns}$ corresponding to 20 RF wavelengths. This allows to have small multi-bunch effects [13]. For CLIC, the long-range wakefields have so far been calculated for one structure only. Therefore $\Delta t = 0.67\,\mathrm{ns}$ is used below.

Particles towards the end of a bunch see decelerating longitudinal fields induced in the accelerating structures by leading particles. The developing correlated energy spread can be partially compensated by accelerating the bunch not on the crest of the RF-wave ($\Phi_{RF} = 0°$) but slightly off-crest. Φ_{RF} has to be limited to avoid inefficiency in the acceleration and large energy variations due to phase jitter, e.g. in the case of CLIC to $\Phi_{RF} \approx 12°$. Full compensation of the energy spread is not feasible, and the beam delivery system is therefore designed to have a very small chromaticity. In CLIC, a final full width energy spread of $\Delta E/E \leq 1\%$ is required.

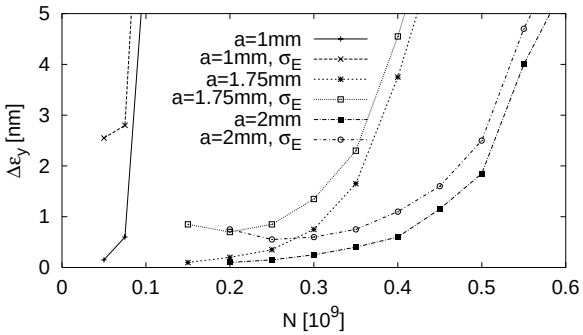

Figure 3: The emittance growth in the CLIC linac as a function of the number of particles per bunch. For each of the three different iris radii a, two cases are shown: no initial energy spread and a constant longitudinal emittance.

With these constraints and for a given structure and gradient G, the minimum bunch length σ_z is determined by N.

4.2 Emittance Preservation

Even in a perfectly aligned linac, transverse beam jitter can result in beam break-up. Leading particles, which have an offset in a structure, induce transverse wakefields, which kick trailing particles in direction of the offset creating a defocusing force. The resulting instability can be avoided by the use of BNS-damping [14]. By varying the RF phase along the linac, an energy spread is introduced in the bunch such that trailing particles have lower energy and are thus focused more strongly by the quadrupoles, thus compensating the wakefield kicks. At the end of the linac the energy spread is reduced. In a strong focusing lattice the energy spread can be smaller than in a weak focusing one; to avoid very large spreads in the linac, one has to choose the former, which also helps to reduce the remaining wakefield effects. However, a strong focusing lattice leads to very tight tolerances for the quadrupole stability.

Static imperfections can lead to a significant vertical emittance growth $\Delta\epsilon_y$ within the linac. The beamline elements can only be positioned to a certain level of accuracy in the tunnel. In the case of CLIC all elements are mounted on girders which are then aligned using a system of wires and lasers. The predicted accuracy for this prealignement is better than about $10\,\mu\mathrm{m}$ [15]. But even this excellent value is not sufficient. Beam-based alignment is necessary. This alignment is based on the assumption that if a small error of

a beamline element has a noticible effect on the beam, this very effect can be measured and the signal used to correct the error.

In CLIC the alignment is performed in three main steps. In the first step the so-called ballistic alignment is applied [16]. First the beam position monitors (BPMs) are aligned, then the quadrupoles, minimising the dispersion in the lattice. In the second step, the RF structures are aligned. The transverse wakefield is measured and minimised by moving the supporting girders. Most of the remaining emittance growth is due to the imperfect measurement of the dipole modes in the structures; the result is still insufficient for our estimated precision of $10\,\mu\mathrm{m}$. Therefore, emittance tuning bumps must be applied; the emittance is measured and minimised globally by moving some structures transversely. Figure 3 shows the emittance growth as a function of N, averaged over 100 machines for the nominal CLIC parameters. Also the results for two structures with smaller irises are shown for comparison. The simulations have been performed with PLACET; for each N, the shortest bunch length has been used, based on the wakefields provided by J.-Y. Raguin [17]. Then RF phases in the linac have been optimised. For each a, a mono-energetic beam has been simulated, then one with an energy spread σ_E consistent with the nominal longitudinal emittance in CLIC ($\sigma_E \propto \sigma_z^{-1}$). The effect of the transverse multi-bunch wakefield is very small and thus not shown. The emittance growth is dominated by two main parameters, the RMS position errors of the BPMs ($10\,\mu\mathrm{m}$) and the precision of the dipole measurement in the structures ($10\,\mu\mathrm{m}$). The optimum structure length L_{cav} depends slightly on N and it is much smaller for $a = 1\,\mathrm{mm}$ than for $a = 2\,\mathrm{mm}$. For a constant number of dipole mode measurement points in each structure, the emittance growth is proportional to the structure length $\Delta\epsilon_y \propto L_{cav}$. In contrast, for the same total number of measurement points in the whole linac, the emittance growth is independent of the structure length. In the simulation, $L_{cav} = 0.5\,\mathrm{m}$ is used throughout to compare at an equal level of instrumentation. At $a = 2\,\mathrm{mm}$, this corresponds to one measurement per structure. At $a = 1\,\mathrm{mm}$, one would have one measurement per four structures; in which case the four structures would need to be built as a single unit.

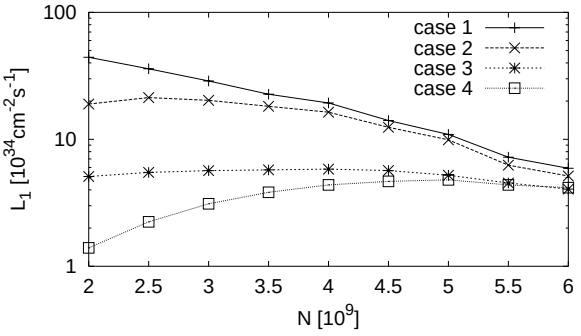

Figure 4: The luminosity as a function of the number of particles per bunch for different assumptions about the emittace contributions $\epsilon_{y,0}$ from other subsystems and the achievable σ_x, see the text.

4.3 Luminosity

First, the luminosity in the peak $\mathcal{L}_1$ is considered for the nominal CLIC structure with $a = 2\,\mathrm{mm}$, including the beam-beam effect. Figure 4 shows $\mathcal{L}_1$ as a function of N. Four different cases are considered. In all of them, the beam-beam effect and the vertical emittance growth in the linac and in the BDS are taken into account. In the first, other sources of emittance are neglected and one uses the optimum σ_x. Smaller N lead to large $\mathcal{L}_1$ in this case. In the second case, a lower limit of $\sigma_x \geq 65\,\mathrm{nm}$ arising from damping ring and BDS is assumed; the achivable $\mathcal{L}_1$ is still largest for an optimum $N \approx 3 \times 10^9$. In the third case, a contribution $\epsilon_{y,0} = 5\,\mathrm{nm}$ in systems other than linac and BDS is accounted for; the luminosity is much lower than in the previous cases with an optimum $N \approx 4\times10^9$. The forth case finally includes both effects with full simulation of the BDS; still the achievable $\mathcal{L}_1$ is larger than the target value. While $N = 5 \times 10^9$ is optimum, the predictions are made for the average emittance growth in the linac, but individual machines differ. Therefore a slightly more conservative $N = 4 \times 10^9$ was chosen and a larger emittance growth is accounted for, which will contain some contribution from dynamics effects.

In Figure 5, $\mathcal{L}_1$ is shown for structures with different a. The variation of the shunt impedance is included and $\epsilon_{y,0} = 5\,\mathrm{nm}$ is always assumed. For each a two cases are shown. In the first, one assumes that the optimum σ_x can be reached, except for $a = 1\,\mathrm{mm}$ where the limit is given by the requirement $\epsilon_x \geq \epsilon_y$. In the second case, $\epsilon_x = 680\,\mathrm{nm}$ is used and the BDS is simulated. In the first case, $\mathcal{L}_1$ is reduced by a factor 2, if $a = 1\,\mathrm{mm}$ is used rather than $a = 2\,\mathrm{mm}$; this may be still bearable. In the second case, almost $\mathcal{L}_1$ is reduced by almost an order of magnitude. Larger a is thus very important, not so much because of the linac beam dynamics but because of the limitation arising from the damping ring and BDS.

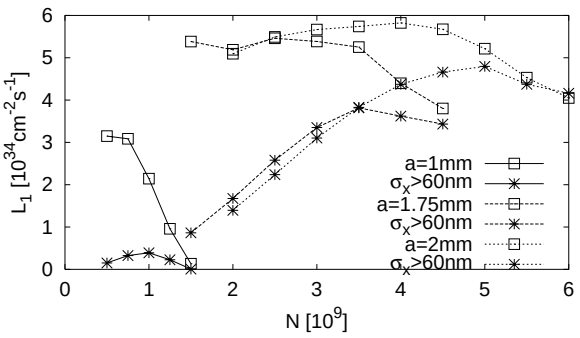

Figure 5: The luminosity as a function of the number of particles per bunch for different iris radii a of the structures.

5 DYNAMIC IMPERFECTIONS

A strong limitation of the performance of a linear collider is expected to come from dynamic imperfections such as ground motion, jitter of the quadrupoles due to cooling water turbulence and variations of the RF phase. These effects can lead to a variation of the transverse beam positions at the IP and also to an increase of the beam sizes. To minimise the emittance growth, position feedbacks are used in the whole machine and in particular at the IP, which steer the beam back to its nominal trajectory.

Ground motion measurements have been performed [18] and some studies are ongoing to measure the vibration of elements (in particular magnets) and the possibility to stabilise them [19, 20, 21]. However the latter investigations are in an early stage and need to be continued. It is very likely that the minimisation of the vibrations of different components has to be taken into account already during the technical design process.

The emittance growth in the main linac due to ground motion can be significant. Using a model of motion measured at CERN [18] one finds that 5 days after beam-based alignment, the emittance growth has doubled, if the beam is steered to remain centred in the BPMs. At this time, more invasive correction techniques have to be applied. Using a model for HERA [18] the time for double the growth would be only one hour. The RMS transverse quadrupole position jitter has to be kept to about $1\,\mathrm{nm}$ in the main linac to avoid more than $6\,\%$ emittance growth.

A random beam-beam offset at the IP with an RMS size of $\langle \Delta y^2 \rangle$ reduces the luminosity, replacing the vertical beam size with the effective beamsize $\sigma_{y,eff} = \sqrt{\sigma_y^2 + 1/2\,\langle \Delta y^2 \rangle}$; the beam-beam forces change the results in detail but not fundamentally. Of special importance is the final quadrupole of the BDS, since its transverse motion translates almost one-to-one into a beam offset. This quadrupole is also difficult to stabilise since it may extend into the detector.

While most feedbacks act from pulse to pulse, an intra-pulse IP feedback could reduce the beam-beam offsets substantially [22]. Such a feedback consists of a BPM and a dipole kicker close to the IP in order to minimise the latency; very fast electronics must be used. Development of such feedbacks is ongoing [23].

6 DAMPING RING

The design of the damping ring poses three main challenges. First, the lattice has to be able to achieve the required low horizontal emittance, even for a low intensity beam. Second, the coupling between the horizontal and vertical plane has to be made small enough to achieve the required vertical emittance. Third, collective effects must be small enough to allow to achieve the required beam intensity. No completely satisfactory solution for the damping ring of CLIC has been found so far. The main problem arises from the intra-beam scattering and the electron cloud effect [24].

It is not clear what is the fundamental limit for the emittance that can be achieved in a damping ring. The value required for CLIC at $E_{cm} = 3\,\mathrm{TeV}$ is difficult to achieve and may be close to the limit. To achieve a constant luminosity one must aim for $\epsilon_x \propto N^2$. A higher N therefore eases the requirement on the low intensity beam damping of the ring because ϵ_x increases. Also the intra-beam scattering should be less critical for a larger beam size. On the other hand, the coupling has to be kept to a lower level at larger bunch charges.

7 CONCLUSION

The design of a multi-TeV linear collider requires many compromises between the requirements of different subsystems. Not all the limitations of these systems are yet fully understood. Thus further simulations and experiments are mandatory to prove that the challenges can be met and that the technology keeps its promises.

8 REFERENCES

[1] E. Accomando et al. Physics Reports. 299(1) (1998).

[2] G.Guignard (ed.). CERN-2000-8.

[3] R. Brinkman, O. Napoly, D. Schulte. PAC 2001.

[4] D. Schulte. CERN/PS 2001-002 (AE) and LCWS 2000.

[5] K. Yokoya and P. Chen, KEK-Prepr.-91-002.

[6] D. Schulte. ICAP 1998.

[7] K. Hirata, K. Oide and B. Zotter, Phys. Lett. B **224** (1989) 437.

[8] R. Assmann, G.A. Blair, H. Burkhardt, A. Faus-Golfe, S. Redaelli, T. Risselada, D. Schulte, W. Wittmer, F. Zimmermann. This conference.

[9] P. Raimondi and A. Seryi, Phys. Rev. Lett. **86** (2001) 3779.

[10] E. D'Amico, G. Guignard, N. Leros, D. Schulte. CERN/PS 2001-028 (AE) and PAC 2001.

[11] W. Wuensch. This conference.

[12] I. Wilson, W. Wuensch. LINAC 2000.

[13] D. Schulte. CERN/PS/98-018 (LP) and EPAC 1998.

[14] V. E. Balakin, A. V. Novokhatsky and V. P. Smirnov, HEACC 1983.

[15] W. Coosemans. Private communication.

[16] T. Raubenheimer and D. Schulte. CERN/PS 99-024 (LP) and PAC 1999.

[17] J.-Y. Raguin. Private communication.

[18] A. Seryi. PAC 2001.

[19] M. Aleksa *et al.*, CERN-SL-2001-045-AP.

[20] S. Allison, L. Eriksson, J. Frisch, L. Hendrickson, T. Himel, K. Luchini and A. Seryi, PAC 2001. PAC 2001.

[21] C. Montag, DESY-M-00-04ZI.

[22] D. Schulte. CERN/PS 2000-051 (AE) and LINAC 2000.

[23] P. N. Burrows, SNOWMASS 2001.

[24] J. Jowett, H. Owen, T. Risselada, F. Zimmermann. CERN-SL-2001-038 and PAC 2001.